

$^{12}\text{C}+^{12}\text{C}$ scattering as the reference system for reaction cross section

Shingo Tagami

Department of Physics, Kyushu University, Fukuoka 819-0395, Japan

Tomotsugu Wakasa

Department of Physics, Kyushu University, Fukuoka 819-0395, Japan

Masanobu Yahiro*

Department of Physics, Kyushu University, Fukuoka 819-0395, Japan

Background: In our previous paper, we tested the chiral (Kyushu) folding model for $^{12}\text{C}+^{12}\text{C}$ scattering, since the profile function in the Glauber mode is constructed for the system. We found that the folding model is reliable for reaction cross sections σ_R in $30 \lesssim E_{\text{lab}} \lesssim 100$ MeV and $250 \lesssim E_{\text{lab}} \lesssim 400$ MeV. Accurate data are available for ^{12}C scattering on ^9Be , ^{12}C , ^{27}Al targets in $30 \lesssim E_{\text{lab}} \lesssim 400$ MeV.

Purpose: We determine matter radius $r_m(\text{exp})$ of ^{12}C from the accurate $\sigma_R(\text{exp})$, using the Kyushu g -matrix folding model.

Results: Our result is $r_m^{12}(\text{exp}) = 2.352 \pm 0.013$ fm for ^{12}C . The model is applied for the accurate data on $^{12}\text{C}+^{27}\text{Al}$ scattering, and yields $r_m(\text{exp}) = 2.936 \pm 0.012$ fm for ^{27}Al .

Conclusion: Our conclusion is that $r_m(\text{exp}) = 2.352 \pm 0.013$ fm agrees with $r_m(\text{exp}) = 2.35 \pm 0.02$ fm determined from interaction cross sections by Tanihata *et al.*

I. INTRODUCTION AND CONCLUSION

Background on experiments and models: We consider that $^{12}\text{C}+^{12}\text{C}$ scattering is the reference system for reaction cross section σ_R , since the profile function in the Glauber mode is constructed for the system; for example, see Ref. [1]. In our previous paper of Ref. [2], we tested the chiral (Kyushu) folding model [3] for $^{12}\text{C}+^{12}\text{C}$ scattering, and found that the folding model is reliable for reaction cross sections σ_R in $30 \lesssim E_{\text{lab}} \lesssim 100$ MeV and $250 \lesssim E_{\text{lab}} \lesssim 400$ MeV by using high-accurate data [4] mentioned below.

Takechi *et al.* measured σ_R for ^{12}C scattering on ^9Be , ^{12}C , ^{27}Al targets in $30 \lesssim E_{\text{lab}} \lesssim 400$ MeV with 2% errors [4]. Thus, high-accurate data are available for $^{12}\text{C}+^{12}\text{C}$, $^{12}\text{C}+^{27}\text{Al}$ scattering in $30 \lesssim E_{\text{lab}} \lesssim 400$ MeV.

Our model is composed of the chiral (Kyushu) g -matrix folding model for scattering [3] and D1S-GHFB+AMP [5] for target densities, where D1S-GHFB+AMP stands for Gogny-D1S HFB with the angular momentum projection (AMP). The Kyushu g -matrix folding model was already applied for $p+^{208}\text{Pb}$ scattering [6]. The model reproduces the data on reactions cross sections σ_R , but not the central values of the data. We then determined a skin value from the data by changing r_{skin} of D1S-GHFB+AMP slightly. Our result $r_{\text{skin}} = 0.278 \pm 0.035$ fm agrees with the recent PREX2 result, i.e., $r_{\text{skin}} = 0.283 \pm 0.071$ fm [7].

In Ref. [8], Kamimura constructed the matter density of ^{12}C for the ground state by using the 3α RGM model; see Table 2 of his paper. The ground state reproduces electron scattering. However, the matter radius $r_m = 2.40$ fm of the ground state is slightly larger than the experimental value $r_m(\text{exp}) = 2.35 \pm 0.02$ fm [9] determined from interaction cross sections by Tanihata *et al.*

Aim: We use the Kyushu folding model, whenever we calculate σ_R . As for $^{12}\text{C}+^{12}\text{C}$ scattering, the σ_R calculated with the phenomenological matter density are compared with those with D1S-GHFB+AMP and 3α RGM. We determine matter radius $r_m(\text{exp})$ of ^{12}C from the accurate data [4].

Results: The σ_R calculated with the phenomenological matter density yield better agreement with the accurate data [4] than those with D1S-GHFB+AMP and the 3α RGM model. We then scale the phenomenological proton and neutron densities and determine $r_m(\text{exp})$ from the accurate data by scaling r_m under the condition that $r_p(\text{scaling}) = r_p(\text{exp})$, where $r_p(\text{scaling})$ ($r_p(\text{exp})$) denotes the scaled (experimental) proton radius. The result thus obtained is $r_m(\text{exp}) = 2.352 \pm 0.013$ fm. The same scaling procedure is used for accurate data [4] on $^{27}\text{Al} + ^{12}\text{C}$ scattering; the result for ^{27}Al is $r_m = 2.936 \pm 0.012$ fm. The reason why we determine $r_m = 2.936 \pm 0.012$ fm for ^{27}Al is not shown in Ref. [10].

Our results are summarized in Table I.

TABLE I. Values of r_p , r_m , neutron radii r_n , r_{skin} . The $r_p(\text{exp})$ are determined from the charge radii [11]. ‘Data’ shows citations on σ_R . The radii are shown in units of fm.

	$r_p(\text{exp})$	$r_m(\text{exp})$	$r_n(\text{exp})$	$r_{\text{skin}}(\text{exp})$	Data
^{12}C	2.3272	2.352 ± 0.013	2.377 ± 0.027	0.050 ± 0.027	[4]
^{27}Al	2.9483	2.936 ± 0.012	2.924 ± 0.023	-0.024 ± 0.023	[4]

Conclusion: Our conclusion is that $r_m(\text{exp}) = 2.352 \pm 0.013$ fm agrees with $r_m(\text{exp}) = 2.35 \pm 0.02$ fm [9] determined from interaction cross sections. We also determine $r_m = 2.936 \pm 0.012$ fm for ^{27}Al from σ_R [4].

* orion093g@gmail.com

II. METHOD

As for the symmetric nuclear matter, Kohno calculated the g matrix by using the Brueckner-Hartree-Fock (BHF) method with chiral $N^3\text{LO}$ 2NFs and NNLO 3NFs [12]. The framework is applied for positive energies. The resulting non-local chiral g matrix is localized into three-range Gaussian forms by using the localization method proposed by the Melbourne group [13, 14]. The resulting local g matrix is referred to as Kyushu g -matrix in this paper [3].

The brief formulation of the double folding model itself is shown below. The potential U consists of the direct part (U^{DR}) and the exchange part (U^{EX}):

$$U^{\text{DR}}(\mathbf{R}) = \sum_{\mu,\nu} \int \rho_{\text{P}}^{\mu}(\mathbf{r}_{\text{P}}) \rho_{\text{T}}^{\nu}(\mathbf{r}_{\text{T}}) g_{\mu\nu}^{\text{DR}}(s; \rho_{\mu\nu}) d\mathbf{r}_{\text{P}} d\mathbf{r}_{\text{T}}, \quad (1)$$

$$U^{\text{EX}}(\mathbf{R}) = \sum_{\mu,\nu} \int \rho_{\text{P}}^{\mu}(\mathbf{r}_{\text{P}}, \mathbf{r}_{\text{P}} - \mathbf{s}) \rho_{\text{T}}^{\nu}(\mathbf{r}_{\text{T}}, \mathbf{r}_{\text{T}} + \mathbf{s}) \times g_{\mu\nu}^{\text{EX}}(s; \rho_{\mu\nu}) \exp[-i\mathbf{K}(\mathbf{R}) \cdot \mathbf{s}/M] d\mathbf{r}_{\text{P}} d\mathbf{r}_{\text{T}}, \quad (2)$$

where $\mathbf{s} = \mathbf{r}_{\text{P}} - \mathbf{r}_{\text{T}} + \mathbf{R}$ for the coordinate \mathbf{R} between P and T. The coordinate \mathbf{r}_{P} (\mathbf{r}_{T}) denotes the location for the interacting nucleon measured from the center-of-mass of the projectile (target). Each of μ and ν corresponds to the z -component of isospin. The original form of U^{EX} is a non-local function of \mathbf{R} , but it has been localized in Eq. (2) with the local semi-classical approximation [15–17] in which P is assumed to propagate as a plane wave with the local momentum $\hbar\mathbf{K}(\mathbf{R})$ within a short range of the nucleon-nucleon interaction, where $M = AA_{\text{T}}/(A + A_{\text{T}})$ for the mass number A (A_{T}) of P (T). The validity of this localization is shown in Ref. [18].

The direct and exchange parts, $g_{\mu\nu}^{\text{DR}}$ and $g_{\mu\nu}^{\text{EX}}$, of the effective nucleon-nucleon interaction (g -matrix) are assumed to depend on the local density

$$\rho_{\mu\nu} = \sigma^{\mu} [\rho_{\text{T}}^{\nu}(\mathbf{r}_{\text{T}} + \mathbf{s}/2) + \rho_{\text{P}}^{\nu}(\mathbf{r}_{\text{P}} - \mathbf{s}/2)] \quad (3)$$

at the midpoint of the interacting nucleon pair, where σ^{μ} is the Pauli matrix of a nucleon in P.

The direct and exchange parts are described by

$$g_{\mu\nu}^{\text{DR}}(s; \rho_{\mu\nu}) = \begin{cases} \frac{1}{4} \sum_S \hat{S}^2 g_{\mu\nu}^{S1}(s; \rho_{\mu\nu}) & ; \text{ for } \mu + \nu = \pm 1 \\ \frac{1}{8} \sum_{S,T} \hat{S}^2 g_{\mu\nu}^{ST}(s; \rho_{\mu\nu}), & ; \text{ for } \mu + \nu = 0 \end{cases} \quad (4)$$

$$g_{\mu\nu}^{\text{EX}}(s; \rho_{\mu\nu}) = \begin{cases} \frac{1}{4} \sum_S (-1)^{S+1} \hat{S}^2 g_{\mu\nu}^{S1}(s; \rho_{\mu\nu}) & ; \text{ for } \mu + \nu = \pm 1 \\ \frac{1}{8} \sum_{S,T} (-1)^{S+T} \hat{S}^2 g_{\mu\nu}^{ST}(s; \rho_{\mu\nu}) & ; \text{ for } \mu + \nu = 0 \end{cases} \quad (5)$$

where $\hat{S} = \sqrt{2S+1}$ and $g_{\mu\nu}^{ST}$ are the spin-isospin components of the g -matrix interaction. As a way of taking the center-of-mass correction to the phenomenological densities of Ref. [19], we use the method of Ref. [20], since the procedure is quite simple. Hamiltonian based on the 3α RGM model has no the center-of-mass coordinate.

In order to deduce the $r_{\text{m}}(\text{exp})$, $r_{\text{n}}(\text{exp})$, $r_{\text{skin}}(\text{exp})$ from measured σ_{R} [4], we have to scale the proton and neutron densities. Now we explain the scaling of density $\rho(\mathbf{r})$. We can obtain the scaled density $\rho_{\text{scaling}}(\mathbf{r})$ from the original density $\rho(\mathbf{r})$ as

$$\rho_{\text{scaling}}(\mathbf{r}) = \frac{1}{\alpha^3} \rho(\mathbf{r}/\alpha) \quad (6)$$

with a scaling factor

$$\alpha = \sqrt{\frac{\langle r^2 \rangle_{\text{scaling}}}{\langle r^2 \rangle}}. \quad (7)$$

III. RESULTS

Figure 1 shows E_{lab} dependence of reaction cross sections σ_{R} for $^{12}\text{C}+^{12}\text{C}$ scattering. The results of the phenomenological projectile and target densities yield better agreement with the data [4] than those of the projectile and target densities based on the 3α RGM model and the D1S-GHFB+AMP projectile and target densities. Eventually, the phenomenological projectile and target densities are best chose for ^{12}C .

The deviation large in the intermediate energies comes from the g -matrix. We do not introduce any fine-tuning factor f , although in Ref. [21] we determined $r_{\text{m}}(\text{exp})$ from $p+^{12}\text{C}$ scattering by using f .

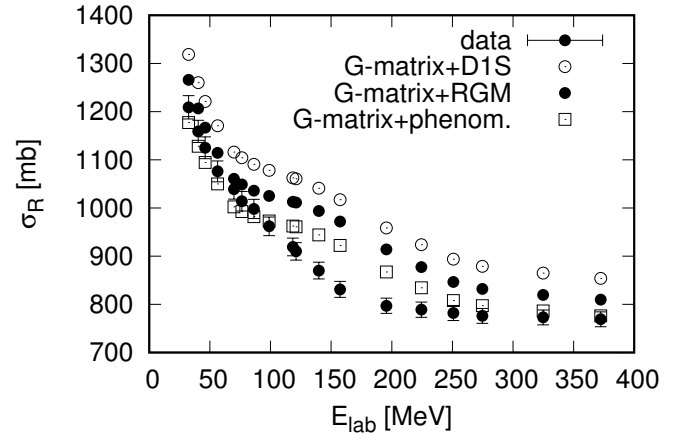


FIG. 1. E_{lab} dependence of reaction cross sections σ_{R} for $^{12}\text{C}+^{12}\text{C}$ scattering. Open circles stand for the results of the D1S-GHFB+AMP projectile and target densities. Closed circles correspond to the projectile and target densities based on the 3α RGM model. Squares denote the results of the phenomenological projectile and target densities. The data are taken from Refs. [4].

This indicates that the phenomenological density is a best choice. Now we determine $r_m(\text{exp})$ from the data in $30 \lesssim E_{\text{lab}} \lesssim 100$ MeV and $250 \lesssim E_{\text{lab}} \lesssim 373$ MeV, scaling the phenomenological projectile and target densities. The result is $r_m(\text{exp}) = 2.352 \pm 0.013$ fm.

The same procedure is taken for $^{27}\text{Al}+^{12}\text{C}$ scattering in $40 \lesssim E_{\text{lab}} \lesssim 87$ MeV and $250 \lesssim E_{\text{lab}} \lesssim 373$ MeV. Our result is $r_m(\text{exp}) = 2.936 \pm 0.012$ fm for ^{27}Al .

IV. DISCUSSIONS

When we solve the Schrödinger equation having U , the symmetrization between P and T is made for $^{12}\text{C}+^{12}\text{C}$ scattering. However, as for $^{27}\text{Al}+^{12}\text{C}$ scattering, the symmetrization is not needed. Table II shows scaling factors, α_n and α_p , for neutron and proton, respectively. In the phenomenological density, the proton density equals the neutron one.

TABLE II. Scaling factors α_n and α_p for neutron and proton.

	α_n	α_p
^{12}C	1.017	0.996
^{27}Al	0.999	0.991

In Ref. [21], we determined $r_m = 2.340 \pm 0.009$ fm from

σ_R of $p+^{12}\text{C}$ scattering by using the fine tuning factor f . In Ref. [10], the experimental values on r_m are accumulated from ^4He to ^{32}Mg . Our result $r_m(\text{exp}) = 2.340 \pm 0.009$ fm is consistent with $r_m(\text{GSI}) = 2.35(2)$ fm of Ref. [9, 10]. The present value with no f agrees with $r_m(\text{GSI}) = 2.35(2)$ fm. This indicates that the present value is more reliable than $r_m = 2.340 \pm 0.009$ fm.

Why the f is necessary for $p+^{12}\text{C}$ but not for $^{12}\text{C}+^{12}\text{C}$? The reason is the following. When one determines $r_m(\text{exp})$ from $\sigma_R(\text{exp})$, one use

$$\sigma_R(\text{exp}) = c_1[r_{m,P}(\text{exp})^2 + r_{m,T}(\text{exp})^2] \quad (8)$$

for $^{12}\text{C}+^{12}\text{C}$ scattering,

$$\sigma_R(\text{exp}) = c_2[r_{m,T}(\text{exp})^2] \quad (9)$$

for $p+^{12}\text{C}$ scattering, where the c_i are constants. These equations are reliable in the case that P and T are black bodies; note that the incident proton is a point-particle. The data σ_R of $p+^{12}\text{C}$ scattering (Fig. 9 of Ref. [21]) are much smaller than that of $^{12}\text{C}+^{12}\text{C}$ scattering (Fig. 1). This indicates that $p+^{12}\text{C}$ scattering is transparent and Eq. (9) is not correct completely.

ACKNOWLEDGEMENTS

We thank Kamimura and Toyokawa for their contributions.

-
- [1] B. Abu-Ibrahim, W. Horiuchi, A. Kohama, and Y. Suzuki, Reaction cross sections of carbon isotopes incident on a proton, Phys. Rev. C **77**, 034607 (2008), [Erratum: Phys.Rev.C 80, 029903 (2009)], arXiv:0710.4193 [nucl-th].
- [2] S. Tagami, M. Tanaka, M. Takechi, M. Fukuda, and M. Yahiro, Chiral g -matrix folding-model approach to reaction cross sections for scattering of ca isotopes on a c target, Phys. Rev. C **101**, 014620 (2020).
- [3] M. Toyokawa, M. Yahiro, T. Matsumoto, and M. Kohno, Effects of chiral three-nucleon forces on ^4He -nucleus scattering in a wide range of incident energies, PTEP **2018**, 023D03 (2018), arXiv:1712.07033 [nucl-th].
- [4] M. Takechi et al., Reaction cross sections at intermediate energies and Fermi-motion effect, Phys. Rev. C **79**, 061601 (2009).
- [5] S. Tagami, M. Tanaka, M. Takechi, M. Fukuda, and M. Yahiro, Chiral g -matrix folding-model approach to reaction cross sections for scattering of Ca isotopes on a C target, Phys. Rev. C **101**, 014620 (2020), arXiv:1911.05417 [nucl-th].
- [6] S. Tagami, T. Wakasa, J. Matsui, M. Yahiro, and M. Takechi, Neutron skin thickness of Pb208 determined from the reaction cross section for proton scattering, Phys. Rev. C **104**, 024606 (2021), arXiv:2010.02450 [nucl-th].
- [7] D. Adhikari et al. (PREX), Accurate Determination of the Neutron Skin Thickness of ^{208}Pb through Parity-Violation in Electron Scattering, Phys. Rev. Lett. **126**, 172502 (2021), arXiv:2102.10767 [nucl-ex].
- [8] M. Kamimura, Transition densities between the $0\ 1\ +$, $2\ 1\ +$, $4\ 1\ +$, $0\ 2\ +$, $2\ 2\ +$, $1\ 1\ -$ and $3\ 1\ -$ states in ^{12}C derived from the three-alpha resonating-group wave functions, Nucl. Phys. A **351**, 456 (1981).
- [9] I. Tanihata, T. Kobayashi, O. Yamakawa, S. Shimoura, K. Ekuni, K. Sugimoto, N. Takahashi, T. Shimoda, and H. Sato, Measurement of Interaction Cross-Sections Using Isotope Beams of Be and B and Isospin Dependence of the Nuclear Radii, Phys. Lett. B **206**, 592 (1988).
- [10] A. Ozawa, T. Suzuki, and I. Tanihata, Nuclear size and related topics, Nucl. Phys. A **693**, 32 (2001).
- [11] I. Angeli and K. P. Marinova, Table of experimental nuclear ground state charge radii: An update, Atom. Data Nucl. Data Tabl. **99**, 69 (2013).
- [12] M. Kohno, Strength of reduced two-body spin-orbit interaction from chiral three-nucleon force, Phys. Rev. C **86**, 061301 (2012), arXiv:1209.5048 [nucl-th].
- [13] H. V. von Geramb et al., Phys. Rev. C **44**, 73 (1991).
- [14] K. Amos and P. J. Dortmans, Phys. Rev. C **49**, 1309 (1994).
- [15] F. A. Brieva and J. R. Rook, Nucl. Phys. **291**, 299 (1977).
- [16] F. A. Brieva and J. R. Rook, Nucl. Phys. **291**, 317 (1977).
- [17] F. A. Brieva and J. R. Rook, Nucl. Phys. **297**, 206 (1978).
- [18] K. Minomo, K. Ogata, M. Kohno, Y. R. Shimizu, and M. Yahiro, The Brieva-Rook Localization of the Microscopic Nucleon-Nucleus Potential, J. Phys. G **37**, 085011 (2010), arXiv:0911.1184 [nucl-th].
- [19] H. de Vries, C. W. de Jager, and C. de Vries, NUCLEAR CHARGE-DENSITY-DISTRIBUTION PARAMETERS, At. Data Nucl. Data Tables **36**, 495 (1987).

- [20] T. Sumi, K. Minomo, S. Tagami, M. Kimura, T. Matsumoto, K. Ogata, Y. R. Shimizu, and M. Yahiro, Deformation of Ne isotopes in the island-of-inversion region, *Phys. Rev. C* **85**, 064613 (2012), arXiv:1201.2497 [nucl-th].
- [21] T. Wakasa, S. Tagami, J. Matsui, M. Takechi, and M. Yahiro, Neutron-skin values and matter and neutron radii determined from reaction cross sections of proton scattering on C12, Ca40,48, Ni58, and Pb208, *Phys. Rev. C* **107**, 024608 (2023), arXiv:2211.16688 [nucl-th].